International Journal of Structural Stability and Dynamics
Vol. 10, No. 3 (2010) 501–527

DOI: 10.1142/S0219455410003592

World Scientific
www.worldscientific.com

ACTIVE VIBRATION CONTROL OF SEISMICALLY EXCITED STRUCTURES BY ATMDS: STABILITY AND PERFORMANCE ROBUSTNESS PERSPECTIVE

ARASH MOHTAT* and AGHIL YOUSEFI-KOMA

Advanced Dynamic and Control Systems Lab (ADCSL)
Faculty of Mechanical Engineering, College of Engineering
University of Tehran, P.O. Box 11155-4563, Tehran, Iran
**amohtat@ut.ac.ir, mohtat_arash@yahoo.com*

EHSAN DEHGHAN-NIRI

Faculty of Civil Engineering, College of Engineering
University of Tehran, P.O. Box 11155-4563, Tehran, Iran

Received 7 April 2009
Revised 14 July 2009

This paper demonstrates the trade-off between nominal performance and robustness in intelligent and conventional structural vibration control schemes; and, proposes a systematic treatment of stability robustness and performance robustness against uncertainty due to structural damage. The adopted control strategies include an intelligent genetic fuzzy logic controller (GFLC) and reduced-order observer-based (ROOB) controllers based on pole-placement and linear quadratic regulator (LQR) conventional schemes. These control strategies are applied to a seismically excited truss bridge structure through an active tuned mass damper (ATMD). Response of the bridge-ATMD control system to earthquake excitation records under nominal and uncertain conditions is analyzed via simulation tests. Based on these results, advantages of exploiting heuristic intelligence in seismic vibration control, as well as some complexities arising in realistic conventional control are highlighted. It has been shown that the coupled effect of spill-over (due to reduction and observation) and mismatch between the mathematical model and the actual plant (due to uncertainty and modeling errors) can destabilize the conventional closed-loop system even if each is alone tolerated. Accordingly, the GFLC proves itself to be the dominant design in terms of the compromise between performance and robustness.

Keywords: Stability robustness; performance robustness; uncertainty due to damage; genetic fuzzy logic controller (GFLC); pole-placement; LQR; bridge-ATMD system.

1. Introduction

Over the last two decades, passive, semi-active and active control strategies have become an integral part of engineering structures for suppressing undesired vibrations due to environmental loads. Currently active control schemes are being

successfully implemented in many real-world full scale structures including buildings, towers and long-span bridges.[1] Tuned mass damper (TMD) systems are vibration control devices that are extensively studied in both passive[2,3] and active[4] applications, because of their efficacy, reliability and low cost. Accordingly, the present investigation utilizes an active tuned mass damper (ATMD) for seismic vibration suppression.

1.1. *Intelligent versus conventional control*

The theory of modern control is well-established and extensively applied with success to structural control. This discipline enables us to achieve optimal performance under nominal conditions for which elaborate mathematical models are derived and control laws are designed. However, it became clear that there is a gap between predicted and realized performance in practice, which increases with increasing dynamical complexity in the system.[5] This gap originating from the lack of reliable detailed knowledge for accurate quantification of a structural system dynamics, along with several other factors such as damage, deterioration and uncertainties, motivates the pursuit of intelligent schemes in structural control. Towards this purpose, fuzzy logic[6] offers an appropriate flexible framework which conveniently handles linguistic synthesis while maintaining required precision for implementation.

Currently, there are numerous investigations available on application of fuzzy logic controllers (FLC) in (semi-) active structural control, e.g. Refs. 7−15. In several instances, fuzzy controllers have been compared against conventional controllers to highlight their advantages. Al-Dawod *et al.*[7] investigated the performance of fuzzy and linear quadratic Gaussian (LQG) control schemes for driving the ATMD force in a 76-storey building benchmark subject to along wind excitation. They concluded that the fuzzy controller performs better than the LQG controller in terms of the building response, the active control force required, the stroke of the actuator, the robustness, and number of sensors required for the system. Pourzeynali *et al.*[11] studied the nominal performance of a genetic fuzzy logic controller (GFLC) for driving an ATMD in comparison with a full-state feedback LQR controller. Guclu and Yazici[15] compared the nominal performance of fuzzy and PD control schemes for vibration control of a building with an ATMD on the top storey and a linear motor on the first one.

In the present investigation, optimal fuzzy logic control is chosen to represent the intelligence in heuristic expert control which is confronted by conventional control represented by pole-placement and LQR schemes. Although optimization of fuzzy logic controllers, as well as many other engineering problems, has been long recognized to be conveniently adaptable to genetic algorithms (GA),[16,17] it is relatively new in the specific field of structural control[8−14] and still several challenges remain. Accordingly, in the present paper, the FLC is optimized through GA implementation. For conventional control, unlike most of the investigations cited in the previous paragraph that compare fuzzy control to rather unrealizable full-state feedback

control of full-order systems, to cope with limitations on sensor measurements and to present a more realistic design, reduced-order control with state observation is employed herein, that shall be denoted as reduced-order observer-based (ROOB) control. Furthermore, most researchers have mainly focused on demonstrating the superior nominal performance of fuzzy controllers while robustness, even if considered, has been less emphasized. However, in this paper, we shall emphasize that the real advantage of fuzzy controllers is not their nominal performance but their superior stability robustness and performance robustness. Indeed, it will be shown that an optimally designed conventional controller, utilizing accurate mathematical model of the linear system, can slightly surpass a fuzzy controller under ideal nominal conditions but might demonstrate significant robustness disadvantages under actual conditions. These robustness disadvantages, especially the instability occurrence, are only revealed if reduction, observation, spill-over and uncertainties are considered in the comparison of conventional controllers with FLCs.

1.2. *Stability and performance robustness to damage uncertainty*

Reducing the response to external disturbances, e.g. earthquake excitations, without catastrophically increasing the effect of uncertainties such as sensor noise and model uncertainty is the primary job of feedback control in structural systems. In designing an active structural control scheme, as well as the nominal performance of the control system, one should be concerned about its robustness against various sources of uncertainty. One of the objectives in this study is to highlight a certain source of model uncertainty that is likely to occur during a natural hazard, namely the uncertainty due to damage or (partly) failure of few structural members. A methodology is proposed to assume some probable damage occurrences, and to conduct simulation tests on designed control systems so as to evaluate their stability robustness and performance robustness against uncertainty in dynamic characteristics of the structure. It will be shown that although the open-loop plant in structural control problems is passively stable, the coupled effect of spill-over (due to reduction and observation) and mismatch between the actual system and the system model utilized in the controller design (due to damage uncertainty) might destabilize the conventional closed-loop control system, even if the isolated effect of each is tolerable for the system. This coupled effect has been less emphasized in the literature, although each issue has been well studied (see Sec. 6.1 for discussion and cited references). The stability and performance robustness of the designed GFLC will also be investigated.

In this paper, the aforementioned control strategies are applied to a seismically excited truss bridge structure. The trade-off between nominal performance and robustness is illustrated and stability robustness and performance robustness of the control schemes against uncertainty due to damage are evaluated through proposed simulation tests. Advantages of employing fuzzy logic in seismic structural control are highlighted, as well as robustness disadvantages arising in realistic conventional

control such as the mentioned instability issues due to the coupled effect of spill-over and uncertainty.

2. Structural Model

2.1. *Structure dynamics*

To illustrate the concepts pursued in this paper, a typical steel truss bridge rather similar to those encountered in practical situations and literature[18] is used as the structural benchmark. The bridge is assumed to be identically excited vertically at its supports due to earthquake. As in Ref. 18, the top chord and bottom chord (including the deck) of the bridge are modeled as beam elements, and the other members as bar elements (see Fig. 1). Table 1 lists the member properties. The dynamic model of this bridge exemplifies the rather generic situation of a seismically excited structure described by a finite dimensional linear time invariant (FDLTI) model derived from finite element (FE) analysis, for which an active vibration control solution is sought.

The equation of motion for the n-DOF (degree of freedom) structure in physical coordinates subjected to ground acceleration $\ddot{y}_g$ can be expressed as:

$$[M_s]\{\ddot{x}(t)\} + [C_s]\{\dot{x}(t)\} + [K_s]\{x(t)\} = -[M_s]\ddot{y}_g\{r\} + \{F_{\text{nodes}}\}, \tag{1}$$

where

- $[\mathbf{M}_s]$, $[\mathbf{K}_s]$ are the structural consistent mass matrix and stiffness matrix in global coordinates obtained after assembling the element matrices and applying the boundary conditions;
- $[\mathbf{C}_s]$ is the proportional damping matrix defined as:

$$[C_s] = \alpha_1[M_s] + \alpha_2[K_s]; \quad \alpha_2 = 2\xi/(\omega_1 + \omega_2), \quad \alpha_1 = \omega_1\omega_2\alpha_2,$$

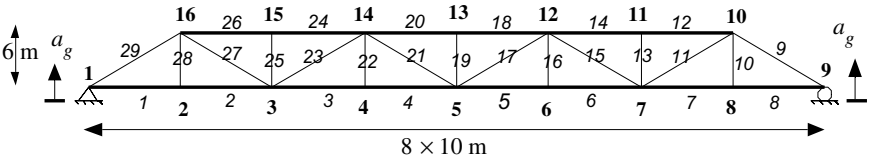

Fig. 1. Bridge FE model.

Table 1. Member properties.

Member Type	Axial Rig. EA (MN)	Flexural Rig. EI (MN.m^4)	Mass ($\times 10^3$ kg/m)
Bottom chord elements	48.5e3	15600	8.9*
Connecting elements	1.25e3	–	0.045
Top chord elements	19.5e3	3100	0.6

*Including mass of the bridge deck.

considering a structural damping of $\xi = 0.02$ and the first and second natural frequencies as ω_1 and ω_2. ($\omega_1 = 6.103$, $\omega_2 = 15.104\,\text{rad/s}$);

- $\{\mathbf{x}(\mathbf{t})\}$ is the global node degrees of freedom defined as

$$\{x(t)\}_{n\times 1} = [\theta_1, \{u_2, v_2, \theta_2\}, \{u_3, v_3, \theta_3\}, \ldots, \{u_I, v_I, \theta_I\}]^T; \quad n = 3I - 3,$$

in which u_i and θ_i 's are the horizontal displacement and rotational freedom of node i respectively; v_i is the relative vertical displacement of the i-th node with respect to the ground; n and I are the total number of degrees of freedom and nodes respectively. For convenience, let us define the notation $\varphi(v_i)$ or φ_i to refer to the DOF number associated with v_i in $\{x(t)\}$, e.g. $\varphi(v_3) = \varphi_3 = 6$ and $x_{\varphi_3} = x_6 = v_3$. This notation will be used in Eqs. (3) and (4).

- $\{\mathbf{r}\}$ is the ground acceleration influence column vector with elements equal to 1 for those associated with vertical displacement (v_i) DOFs, and 0 for the rest. This vector accounts for the vertical acceleration terms which must be written in the absolute reference frame, i.e. $\ddot{v}_i + \ddot{y}_g$.
- $\{\mathbf{F}_{\text{nodes}}\}$ is the column vector of generalized external forces exerted on the nodes (the control forces on specific nodes will be inserted here).

2.2. *ATMD modeling/installation*

In this investigation, the active tuned mass damper (ATMD) consisting of a TMD attached to the bottom side of the bridge deck, and a linear force actuator installed between the deck and the TMD mass is utilized to apply the control action. Now, we shall derive the formulation of the combined structure-controller, assuming that the ATMD is installed to the i-th node on the bottom chord of the truss bridge as shown in Fig. 2.

The equation of motion for the TMD can be written as:

$$m_T(\ddot{y}_T + \ddot{y}_g) = -F_{yi} = -[F_{\text{act}} + k_T(y_T - v_i) + c_T(\dot{y}_T - \dot{v}_i)], \tag{2}$$

where the subscript T refers to the TMD, F_{act} refers to the actuator (active control) force and F_{yi} is the total upward force exerted on node i of the structure (with $-F_{yi}$ acting on the TMD). A direct modification of the matrices in Eq. (1) by adding

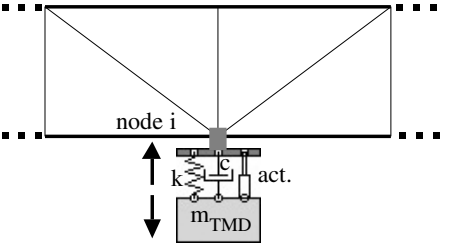

Fig. 2. ATMD physical installation.

Eq. (2) yields the combined structure-ATMD dynamic equation of motion as:

$$[M_m]\begin{Bmatrix}\{\ddot{x}(t)\}\\ \ddot{y}_T\end{Bmatrix}+[C_m]\begin{Bmatrix}\{\dot{x}(t)\}\\ \dot{y}_T\end{Bmatrix}+[K_m]\begin{Bmatrix}\{x(t)\}\\ y_T\end{Bmatrix}=-[M_m]\ddot{y}_g\begin{Bmatrix}\{r\}\\ 1\end{Bmatrix}+\begin{Bmatrix}\{\vec{F}_{\text{nodes}}\}\\ -F_{\text{act}}\end{Bmatrix}, \tag{3}$$

where:

$$M_m=\begin{bmatrix}M_{s_{n\times n}} & 0_{n\times 1}\\ 0_{1\times n} & m_T\end{bmatrix}_{(n+1)\times(n+1)}$$

$$C_m=\begin{bmatrix}C_{s_{n\times n}} & 0_{n\times 1}\\ 0_{1\times n} & c_T\end{bmatrix}+C^*_{(n+1)\times(n+1)};\quad C^*=[C^*_{l,p}]=\begin{cases}c_T & l=p=\varphi(v_i)\\ -c_T & l=\varphi(v_i),p=n+1\\ -c_T & l=n+1,p=\varphi(v_i)\\ 0 & \text{otherwise}\end{cases},$$

$$\{F_{\text{nodes}}\}=\{f_l\}_{n\times 1}=\begin{cases}+F_{\text{act}} & l=\varphi(v_i)\\ 0 & \text{otherwise (assumming no external force)}\end{cases}$$

with K similarly modified to K_m as C_m.

Now, let us define the combined structure-ATMD dynamic system as shown in Fig. 3 with the representative nodes i and j as the input (ATMD location) and output (displacement and velocity sensors) nodes, respectively.

The state-space representation for the combined (subscript C) system shown in Fig. 3 can be written as:

$$\begin{aligned}\dot{Z}_C &= A_C Z_C + B_C U_C\\ Y_C &= C_C Z_C + D_C U_C,\end{aligned} \tag{4-I}$$

with the state variable, input and output vectors:

$$Z_C=\begin{Bmatrix}\{x(t)\}\\ y_T(t)\\ \{\dot{x}(t)\}\\ \dot{y}_T\end{Bmatrix}_{N\times 1},\quad U_C=\begin{Bmatrix}\ddot{y}_g\\ F_{act}\end{Bmatrix}_{2\times 1},\quad Y_C=\begin{Bmatrix}v_j\\ \dot{v}_j\end{Bmatrix}_{2\times 1}, \tag{4-II}$$

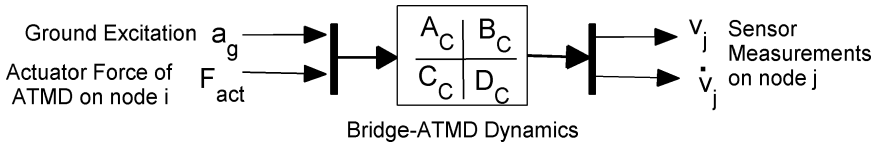

Fig. 3. Bridge-ATMD dynamic system.

and the associated matrices written as:

$$
\begin{aligned}
A_c &= \begin{bmatrix} 0_{(n+1)\times(n+1)} & I_{(n+1)(n+1)} \\ -M_m^{-1}K_m & -M_m^{-1}C_m \end{bmatrix}_{N\times N}, \\
B_C &= \begin{bmatrix} 0_{(n+1)\times 2} \\ \begin{Bmatrix} -r \\ -1 \end{Bmatrix} B_{2,2} \end{bmatrix}_{N\times 2} \quad ; \quad B_{2,2} = \{M_m^{-1}(:,\varphi_i) - M_m^{-1}(:,n+1)\}, \\
C_C &= [c_{l,p}]_{2\times N} = \begin{cases} 1 & l=1, p=\varphi_j \\ 1 & l=2, p=\varphi_j+n+1\,, \\ 0 & \text{otherwise} \end{cases} \quad D_C = 0_{2\times 2},
\end{aligned}
\tag{4-III}
$$

where $N = 2n + 2$ is the total number of states, and $M_m^{-1}(:,\varphi_i)$ and $M_m^{-1}(:,n+1)$ refer to the ϕ_i-th and $(n+1)$-th columns of M_m^{-1}.

By utilizing the generalized input-output formulation derived, any desired configuration of TMDs can be installed on the truss bridge with arbitrary sensor measurements. The optimal distribution/placement of actuators has been studied by many researchers. Ref. 19 is an interesting case in point. For the present case, considering the structure, load and symmetry causing the first vibrational mode of the structure to be most significantly excited, a single ATMD installation at the mid-span node is a simple but rather effective solution.

2.3. *Passive control*

As mentioned previously, a TMD installation at the mid-span node is applied in this investigation. The TMD main structural parameters are its mass, stiffness and damping defined as:

$$
m_T = \mu \times m_{total}, \quad k_T = m_T(\beta\omega_1)^2, \quad c_T = 2\xi_T\sqrt{m_T k_T}, \tag{5}
$$

in terms of TMD tuning parameters μ, β and ξ_T. The total mass ratio is fixed as $\mu = 0.03$ throughout this study while the TMD frequency ratio β and damping ratio ξ_T shall be optimized. The optimization is based on the minimization of the worst case dynamic magnification factor (DMF), i.e. the H_∞ norm of the transfer function from excitation input to structural response. Although closed-form solutions for min. max. DMF optimization of single DOF structure-TMD systems are reported in the literature, e.g. Ref. 20, we shall propose a simple numerical optimization scheme to be applied to the structure as a whole (not only a single mode). The scheme involves utilizing a GA optimizer to find β and ξ_T with the peak amplitude of the frequency response from a_g to v_5 as the objective to be minimized. This yields values of $\beta = 0.93$ and $\xi_T = 0.14$ as optimal tuning parameters. As it can be seen from Fig. 8, the addition of the TMD breaks down the peak amplitude of the frequency response by introducing a secondary peak, which in case of optimality will be equal to the reduced primary peak.

2.4. *Reduced-order system*

A reduced-order system (ROS) is derived from the original structure-ATMD system, referred to as the full-order system (FOS), but involves a smaller number of DOF for the purpose of controller design as will explained later. There are many system reduction schemes available in the literature.[21–23] A state reduced-order system (SROS), as adopted in this investigation, is obtained by evaluating and truncating the least important states. The truncation error can be measured in terms of the peak gain across frequency, i.e. the H∞ norm. The error bounds are function of the neglected Hankel singular values which define the energy of each state in the system. For the state-space system (4), the Hankel singular values can be mathematically defined as:

$$\sigma_H = \sqrt{\lambda_i(PQ)}; \quad i = 1, 2, \ldots, N, \tag{6}$$

where N is the number of states of the system (4–III), while P and Q are controllability and observability grammians satisfying the following relations:

$$A_C P + P A_C^T = -B_C B_C^T, \quad A_C^T Q + Q A_C = -C_C^T C_C.$$

Keeping larger energy states of a system preserves most of its characteristics in terms of stability, frequency and time responses. So an ROS of order 8 seems to be adequate as deduced from Fig. 4 and will be denoted as:

$$\begin{aligned} \dot{x} &= [A_r]x + [B_r^g | B_r^F] \begin{Bmatrix} \ddot{y}_g \\ F_{\text{act}} \end{Bmatrix} \\ y &= [C_r]x + [D_r^g | D_r^F] \begin{Bmatrix} \ddot{y}_g \\ F_{\text{act}} \end{Bmatrix} \end{aligned}. \tag{7}$$

This ROS will be used only for the reduced-order control design of Secs. 3.1 and 3.2. All performance evaluation and validations will be carried out by applying the designed control schemes on the FOS.

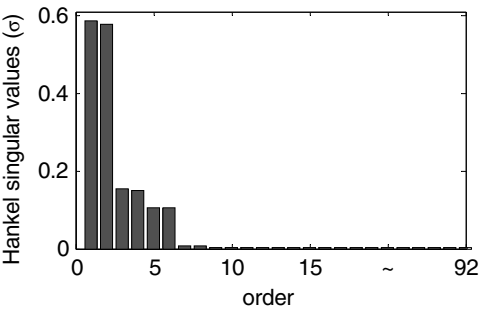

Fig. 4. Hankel singular values plot.

2.5. *Problem-definition for active control*

In designing an active control strategy, the objective is to reduce the structural response under limitations on both the control force level and the number of measured signals imposed by the available actuator(s), power supply and sensors. A maximum allowable control effort of 500 kN is assumed along with two available sensor measurements. The controller performance is evaluated in terms of its ability to attenuate maximum displacement response as a measure of structural safety. An additional criterion would be the controller efficiency in mitigating the root mean square (rms) displacement response. Towards this end, the following weighted average indices seem appropriate:

$$I = \frac{\sum_{r=\text{earthquakes}} w_r P_r}{\sum_r w_r}; \quad P_r = (\max(v_5^{\text{Ctrl}})/\max(v_5^{\text{Unctrl}}))_{\text{earthquake r}}, \tag{8-I}$$

$$\tilde{I} = \frac{\sum_{r=\text{earthquakes}} w_r R_r}{\sum_r w_r}; \quad R_r = (\text{rms}(v_5^{\text{Ctrl}})/\text{rms}(v_5^{\text{Unctrl}}))_{\text{earthquake r}}, \tag{8-II}$$

where P_r and R_r are the performance ratio (controlled to uncontrolled peak displacement response) and the rms ratio (controlled to uncontrolled rms displacement response) computed from earthquake record r; and, w_r is the weighting coefficient associated with earthquake r. Three earthquake records, namely El Centro, 18 May 1940; Kobe, 17 Jan 1995; Northridge, 17 Jan 1994 have been considered with peak ground accelerations (PGA) of 0.343, 0.818 and 0.827 ($\times g$) as the weighting coefficients. These earthquake signals including near-field and far-field records are frequently used in the literature and shall be employed in this investigation for the purpose of training (optimally tuning) the genetic fuzzy logic controller (GFLC) and evaluating the aforementioned indices. In design problems for practical implementation, the methodology illustrated in this investigation can be applied using more seismological records from the site of implementation.

3. Controller Design by Pole Placement/LQR

The key idea of feedback control laws in state-space is to utilize the measurement of the current state of the system (or its estimation) to generate an actuator control signal. A full state feedback law for the full order system might be neither easy to design due to the complexity involved, nor feasible to be realized due to the large number of required measurements. In this study to cope with the limitations on sensor measurements and to present a more realistic design, reduced-order observer-based (ROOB) control has been studied. The pole-placement and LQR techniques are convenient methods to determine the gain matrix in feedback laws, with classical application in structural control (see e.g. Refs. 22, 24, 25). The control law design adopted here incorporates the following steps:

(1) Determining the gain matrix K for full-state feedback control of the ROS.

(2) Designing a dynamic observer to estimate the state of the ROS using only two sensor measurements.
(3) Employing the designed control scheme on the FOS to evaluate its performance and to test the possible undesirable spill-over effects.

3.1. *State feedback law*

Let us consider a full state feedback closed-loop regulator system for the ROS (7) as shown in Fig. 5.

It can be easily shown[26] that if and only if the system (7) is completely state controllable, the poles of the closed-loop system shown in Fig. 5 can be arbitrarily placed through appropriate determination of the matrix K. The feedback gain matrix K that forces the eigen values of $A_r - B_r^F K$ to be placed at $\mu_1, \mu_2, \ldots, \mu_n$ (the desired poles for the closed-loop system) leading to a characteristic equation of

$$\begin{aligned}\phi(s) &= |sI - A_r + B_r^F K| = (s-\mu_1)(s-\mu_2)\cdots(s-\mu_n)\\ &= s^n + \alpha_1 s^{n-1} + \cdots + \alpha_{n-1}s + \alpha_n = 0,\end{aligned}$$

can be obtained using the Ackermann's formula, which can be written as[26]:

$$K = [0 \quad 0 \quad \cdots \quad 0 \quad 1][B_r^F \quad | \quad A_r B_r^F \quad |\cdots| \quad A_r^{n-1} B_r^F]^{-1}\phi(A_r). \tag{9}$$

The poles of the closed-loop system can be judiciously placed using classic control insight, graphic inspection and some trial-and-error. There are also a number of proposed methods and guidelines for pole selection that can be found in the literature; e.g. Wang *et al.*[25] propose moving around the prescribed closed-loop eigen values so that some other control objective(s) can be met. In this paper, a representative placement of poles that delivers high nominal performance is utilized for the purpose of comparison with other control schemes (to show the trade-off between nominal performance and robustness in different control designs, this specific pole-placement design represents the extreme of high performance but poor robustness). The poles are placed to give an improved damping to the poles with a slight modification of natural frequencies as shown in Fig. 6.

Although mathematically realizable, any arbitrary dramatic modification of the closed loop poles may not be allowable in terms of control effort and final performance

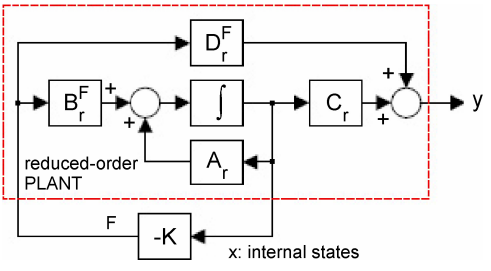

Fig. 5. State feedback control of ROS.

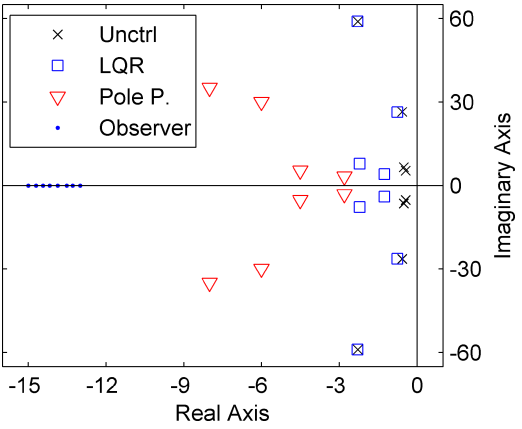

Fig. 6. Poles arrangement for uncontrolled (Unctrl), LQR, pole-placement systems and observer.

results. Thus, the saturation action must be included in the simulation for verifications of results. In this study, the feedback laws are designed so as the saturation action is negligible at least for the earthquakes considered, in order to avoid nonlinearities.

Alternatively, in the LQR method, the matrix K is determined so as to minimize the performance index:

$$J = \int_0^\infty (y^T Q y + u^T R u) dt. \tag{10}$$

The solution for K can be found after solving a Ricatti equation.[26] Considering the force input and the deflection v_5 as the only output, Q and R would be scalars balancing the compromise between response reduction and control effort. Here the ratio R/Q is set to 1e-14 by trial and error to produce maximum performance while keeping the saturation action acceptable under the earthquake records considered.

3.2. *Dynamic observer*

Referring to Eq. (7), a mathematical model for an observer which utilizes the measurement $y = v_5$ and control command F_{act} to estimate n_r internal states of the ROS might be written as follows:

$$\dot{\tilde{x}} = A_r \tilde{x} + B_r^F F_{\text{act}} + K_e(y - C_r \tilde{x} - D_r^F F_{\text{act}}). \tag{11}$$

The substitution of y from the second equation of (7) into Eq. (11) and by defining the observation error e as $x - \tilde{x}$, yields:

$$\dot{e} = (A_r - K_e C_r)e + (B_r^g - K_e D_r^g)\ddot{y}_g. \tag{12}$$

In order for the observer to demonstrate acceptable performance, the poles of $A_r - K_e C_r$ must be stable and highly damped. Besides, for acceptable disturbance-error

rejection the second term in Eq. (12) must be eliminated. To achieve these two goals, we shall feed the observer by an additional accelerometer measurement from the ground (bridge supports) excitation and define the observer as:

$$\begin{aligned}\dot{\tilde{x}} &= (A_r - K_e C_r)\tilde{x} + [B_r^g - K_e D_r^g | B_r^F - K_e D_r^F | K_e] \begin{Bmatrix} \ddot{y}_g \\ F_{\text{act}} \\ v_5 \end{Bmatrix} \\ \tilde{y} &= \tilde{x} = I_{n_r \times n_r} \tilde{x} + 0.\end{aligned} \tag{13}$$

The closed-loop system with the designed observer is sketched in Fig. 7.

Notice that by the separation principle, the closed-loop poles of the observed-state feedback control consist of the poles due to the feedback law $F = -Kx$ alone and the poles due to the observer design alone. Hence by choosing the observer poles sufficiently faster than the controller poles, the effect of addition of the observer on the closed-loop system will be negligible. Once the observer poles have been chosen (as depicted in Fig. 6), the observer gain matrix K_e can be determined using the pole placement technique based on the duality between controllability and observability.[26]

3.3. *Performance of control strategies on FOS*

Since the controllers are designed based on the ROS, they may excite the unselected (or residual) modes in the FOS. This effect is referred to as the control spillover. Further the feedback measurement contains contribution from the residual modes, which will influence the control performance. This is referred to as the observation spillover.[22]

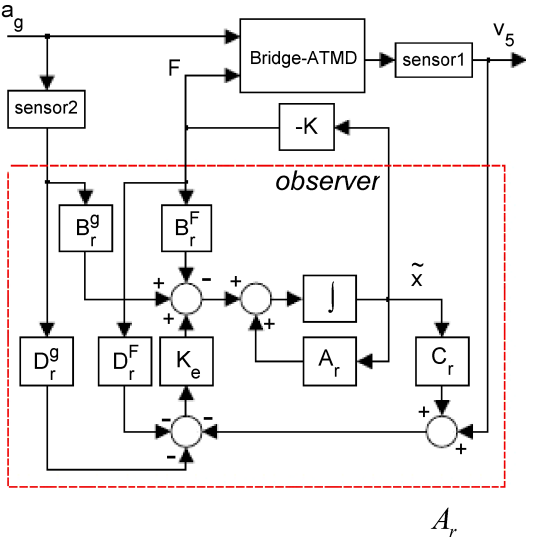

Fig. 7. Closed-loop configuration with dynamic observer.

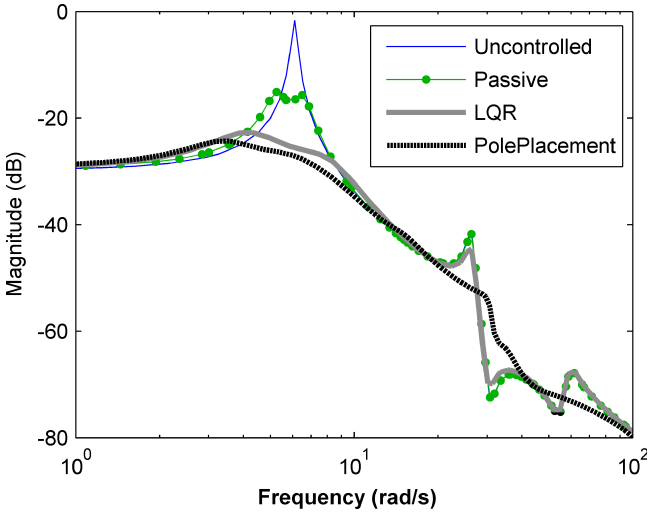

Fig. 8. Frequency response comparison.

The control systems (controller + observer) designed in the previous sections shall be applied to the closed-loop with the FOS to numerically investigate the performance and coupled spillover effects. Figure 8 compares the frequency response of the uncontrolled, TMD, LQR and pole placement FOS configurations to ground excitation. The frequency responses of the ROOB LQR and pole placement control schemes applied to the FOS in the frequency range shown in Fig. 8, closely match those predicted by the reduced-order control design, i.e. the spillover effects have negligible influence on nominal performance. Indeed the robustness issues due to spill-over instabilities of higher frequency modes, is what we should be concerned about, see Sec. 6.1 for a more detailed discussion.

4. GFLC Design

Introduced by Lotfi Zadeh[6] in 1965, the fuzzy theory has been extensively investigated for structural control.[7–15] Fuzzy controllers have been recently implemented in real-world structures, e.g. the two long-span Nakajima and Kurushima bridges[1] in Japan. The main advantages of fuzzy control scheme are its inherent robustness to uncertainties of input data and sensor noises, and its ability to handle nonlinearities without significant modifications as a consequence of the fuzzy logic and linguistic synthesis nature. Fuzzy controllers can be designed based on human experience and knowledge. This makes the fuzzy logic control scheme a mathematical model-free approach. The knowledge base identifies the actual variables driving the control process; thus, only this significant variables need to be measured and fed to the FLC. The whole fuzzy controller can be easily implemented in a fuzzy chip. Moreover, the FLC can be adaptive by modifying its rules and membership functions and employing

training techniques. Fuzzy logic can also be adopted for a variety of other structural control applications such as supervisory over several sub-controllers or modeling the nonlinear dynamic behavior of structural elements. Ref. 13 provides an intriguing combination where Sugeno-type fuzzy inference is used for modeling MR dampers and Mamdani-type fuzzy logic is used to control them.

4.1. *Fuzzy control*

A FLC is incorporated into a closed-loop control system similar to conventional controllers as shown in Fig. 10 for the case of the present implementation. As it can be seen from this figure a FLC consists of the following components:

Fuzzification: The sensor measurements (in this study v_5 and $\dot{v}_5$), as controller input variables, are fuzzified into linguistic terms using membership functions of input variables stored in the knowledge base.

Knowledge base: The knowledge base consists of fuzzy *IF-THEN* rules and membership functions. In this investigation, the FLC is designed using two input variables and one output variable, with IF-THEN rules of the form:

$$M^i : \text{if} \;\; x_1 = A_i \quad \text{and} \quad x_2 = B_i \;\; \text{then} \;\; y = C_i. \tag{14}$$

There is no general method to define the fuzzy rules, indeed it is based on human expertise and logical reasoning and may need some trial and error. Of course, some efforts to mechanize the fuzzy rules generation are reported in the literature, such as the self-organizing fuzzy logic controller (SOFLC)[27] and the *learning from examples* scheme.[28] The fuzzy rules used in this investigation which constitute a fuzzy associative memory (FAM) to map the FLC inputs onto its output are adopted from Ref. 11 and presented in Table 2.

The FLC has been designed using five bell shape membership functions for each input variable (displacement and velocity of the mid-span node of the bridge relative to the ground) and seven membership functions for output command. The input subsets are: LP, P, Z, N, and LN; while the output subsets are: PL, PM, PS, ZR, NL, NM, and NS; with the well-known linguistic abbreviations: P = Positive; N = Negative; Z or ZR = ZeRo; L = Large; M = Medium and S = Small.

Table 2. Fuzzy rules (FAM).

v_5	$\dot{v}_5$ (Velocity)				
(Displacement)	LN	N	Z	P	LP
LP	NS	NS	NM	NL	NL
P	NS	NM	NM	NM	NL
Z	PS	ZR	ZR	ZR	NS
N	PL	PM	PM	PM	PS
LN	PL	PL	PM	PS	PS

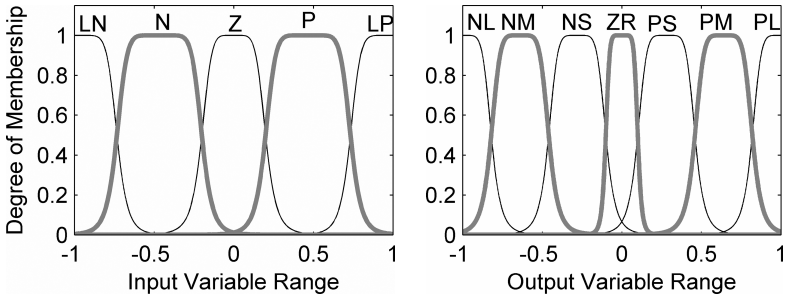

(a) (b)

Fig. 9. Normalized input (a)output (b) membership functions.

As illustrated in Fig. 9, generalized bell shape functions of the form:

$$\mu_x = \frac{1}{1 + |x - c/a|^{2b}} \tag{15}$$

have been used, where a is the half-width at 0.5 membership grade, b defines the slope of the membership function and c is the center position of the membership function. This can approximate almost all other types of membership functions based on its rather few parameters.[8]

Fuzzy inference: This unit is the fuzzy reasoning (decision-making) component, which performs various fuzzy logic operations to infer the control action for a given fuzzy input.

Defuzzification: The inferred fuzzy control action is converted into required crisp control value in this unit.

The specifications of the FLC used in this study are summarized in Table 3.

Although, the process of designing a FLC relies on expert knowledge, the utilization of an optimization scheme can greatly simplify the trial-and-error process and enhance the FLC performance on the specific structural plant under active control. This will be discussed in what follows.

Table 3. FLC specifications.

Parameters	Variables/Operator
Input variables	Displacement v_5 (5 subsets) Velocity $\dot{v}_5$ (5 subsets)
Output variables	Control signal (7 subsets)
Aggregation	Maximum
Fuzzy inference	Mamdani[30]
Defuzzification	Center of gravity (COG)

4.2. *Optimizing the FLC by GA*

GA being a soft computing algorithm can be conveniently implemented to many engineering optimization problems with a most appealing advantage of having better chance of convergence to a near-global optimum. In the structural control literature, genetic algorithms have been applied in many optimization problems: from passive vibration control, e.g. Ref. 29, to semi-active or active vibration control by fuzzy logic controllers[8−14]; and the current study continues this trend of research.

Figure 10 clearly illustrates the implementation of GA for the purpose of optimizing the FLC in this investigation. This figure presents an overview of GA internal algorithm (for details concerning GA internal algorithm the corresponding abundant literature can be consulted, e.g. see Ref. 31) along with its interaction with the simulation and the iterations required to achieve the optimized solution. '$Run(i, r)$' in the figure, refers to the simulation-run required for the evaluation of the controller performance ratio (p_r^i) associated with the ith individual of the gth generation

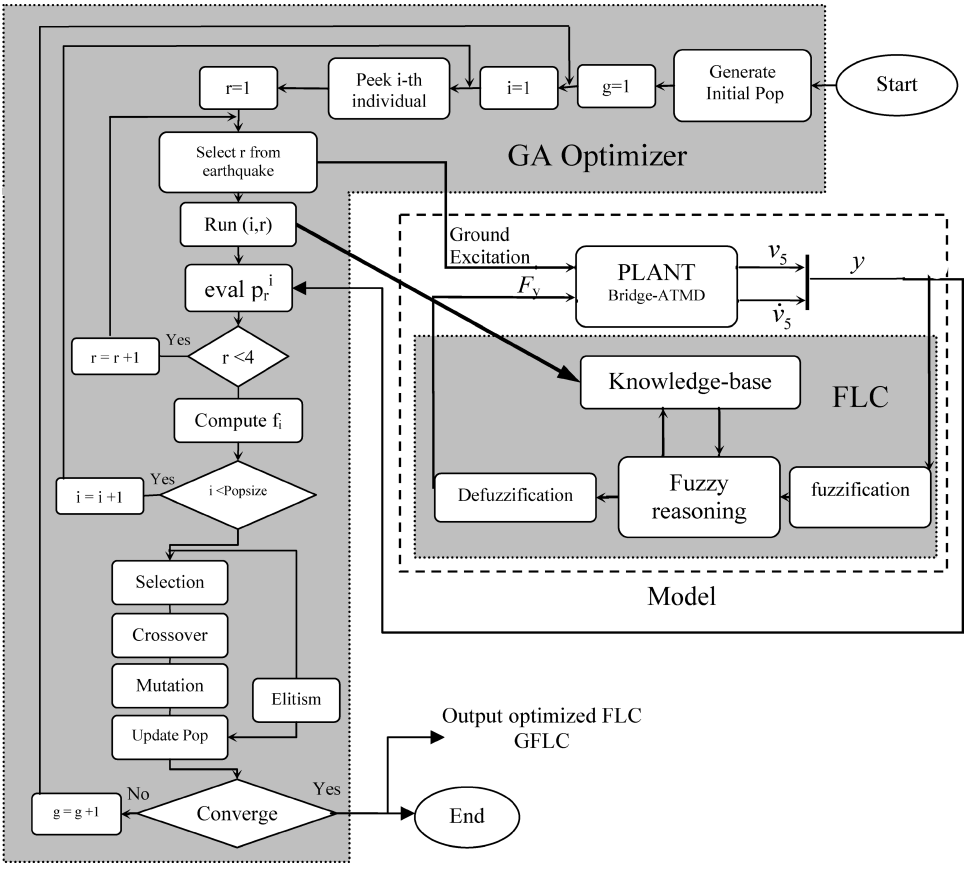

Fig. 10. GA-optimizer interaction with fuzzy controlled system for GFLC design.

subjected to the r-th earthquake loading. An appropriate maximization fitness for the ith individual, computed based on the index (8-I), might be formulated as:

$$f_i = (1 + I_i)^{-1}; \quad I_i = \sum_r w_r p_r^i / \sum_r w_r. \tag{16}$$

In this study, the design variables of the controller to be optimized are the membership functions parameters a, b, c for the inputs and output along with the TMD tuning parameters ξ_T, β. Bearing in mind the symmetry of the membership functions and fixing the center position c of the extreme subsets, we would have 24 membership tuning parameters that along with the TMD tuning parameters would be concatenated to form a chromosome. Owing to the large number of design variables and simulations required, some care should be taken on the GA-implementation to gain better chance of convergence to a near global optimum:

(1) The GA can be set to search the optimum combination of membership tuning parameters within appropriate restricted range for each parameter. This shrinks the design space and makes GA yield reasonably-shaped membership functions.
(2) Reasonable and significant accuracy should be dedicated to each parameter to control the string length of each chromosome in the GA implementation.
(3) The rates of exploration and exploitation must be balanced in the GA run. Cross-over and mutation probabilities are two decisive parameters in this regard.

The specifications of the GA implementation applied are presented in Table 4.

5. Nominal Performance of Designed Control Schemes

The performance of the designed control schemes on the nominal full-order plant might be evaluated using simulation to obtain the dynamic response of the control system to the aforementioned earthquake records. Figure 11 shows the time histories of displacement response of the controlled systems to El-Centro and Kobe earthquakes. The simulation results for nominal performance evaluation of the control schemes (TMD, pole-placement, LQR and GFLC) has been reported in Table 5 in

Table 4. GA optimization.

GA/Operator options	Value/Setting
Population size	100
Generations	90
Selection	
Type	Proportionate (RWS)
Fitness	f_i (Eq. 16)
Cross-over	
Type	Two-point
Prob.	0.7
Mutation Prob.	0.03
Elitism	2 per generation

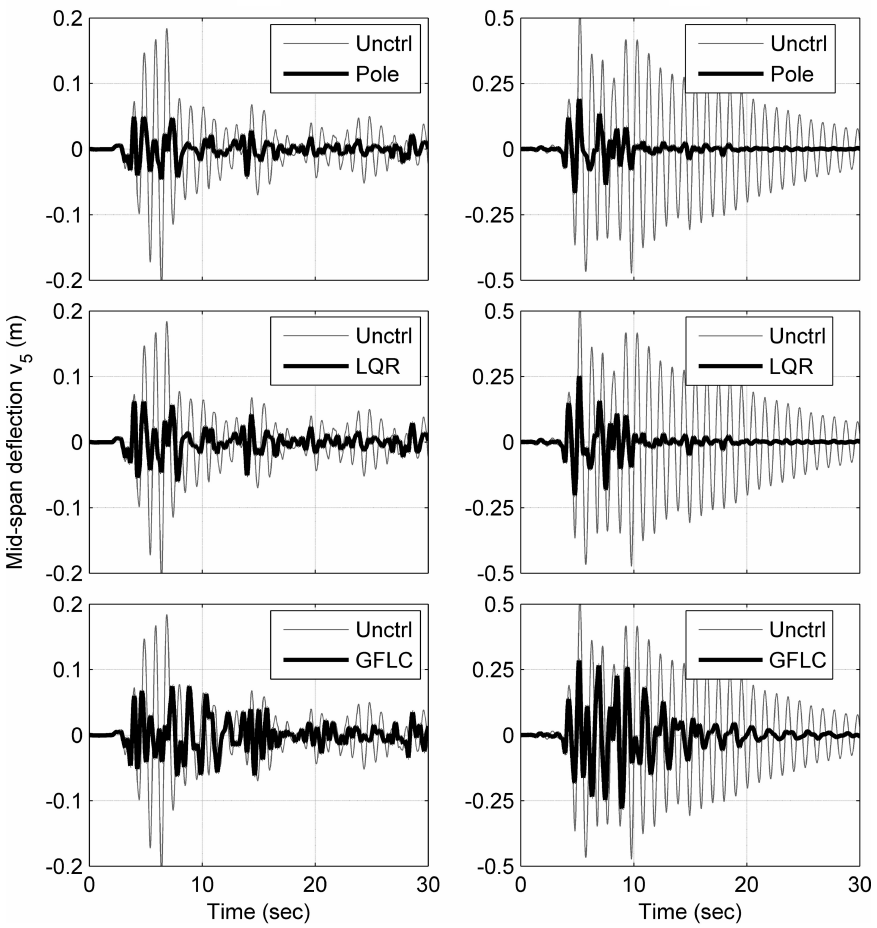

Fig. 11. Comparison of displacement-response time-histories to El-centro(a) & Kobe(b).

Table 5. Nominal performance data.

Loading	Performance[a][b]				Response[c][d] Unctrl
	TMD	Pole Place	LQR	GFLC	
El-Centro	0.610	0.235	0.291	0.349	212
	0.647	0.279	0.341	0.464	36.6
Kobe	0.866	0.463	0.512	0.534	529
	0.442	0.198	0.245	0.423	144
North Ridge	0.970	0.637	0.651	0.651	320
	0.629	0.375	0.448	0.599	78.2
Weighted Ave.	0.865	0.496	0.532	0.551	
	0.555	.286	0.346	0.503	

Note: (a) Performance ratio Eq. (8-I), (b) rms ratio Eq. (8-II), (c) displacement peak (mm), (d) displacement rms (mm).

terms of the performance and rms ratios associated with each considered earthquake and the weighted performance indices (8-I, 8-II). The displacement peak and rms values for each control case in response to each earthquake record can be obtained through multiplication of the associated ratio by the respective response reported in the last column. As can be concluded from these results, the controller designed by pole-placement delivers the best nominal performance. Nevertheless, all controllers perform rather comparably.

6. Robustness Against Uncertainty Due to Damage

By robustness analysis, we mean evaluating the sensitivity and endurance of a control scheme in terms of its ability to maintain stability (stability robustness) and meet the performance requirements (performance robustness) in the presence of uncertainties.

In this paper, we propose the analysis of robustness against uncertainty due to damage by subjecting the designed control schemes to some robustness tests. The robustness tests developed here involve two cases. The first case is a 30% reduction in the stiffness of the two members 9 and 29, the mostly stressed truss members in Fig. 1, due to damage and the second is the case of complete failure of these two members. The former causes a 5.3% and the latter a 30.7% reduction in the first natural frequency of the structure. These are two representative damage scenarios to evaluate the robustness of the control schemes against uncertainty in dynamic characteristics of the structure.

6.1. *Stability robustness*

The primary concern in active control is stability. Even if the control system fails to perform as intended, instability occurrence due to probable uncertainties is unacceptable. Stability is a basic property of closed-loop systems with several well-established mathematical criteria for conventional controllers[26] but only few available methods for fuzzy controllers.[32]

The stability of conventional linear control schemes can be easily verified through analysis of closed-loop poles. The closed-loop poles of the structure-ATMD system controlled by ROOB pole-placement and LQR are shown in Figs. 12 and 13. As can be observed from the unstable poles, the specific LQR and pole-placement control systems designed, although nominally performing similarly, have quite different levels of stability robustness. Indeed, the specific controller designed by pole-placement is much more vulnerable to uncertainty, as its poles are more easily pushed to the right half-plane by structural damage.

It has been shown that the estimation error and state dynamics are designed stable and remain uncoupled when the actual system and the mathematical model utilized to design the observer-based feedback controller are the same; but, once reduction (for control design) and structural damage get involved, instability might

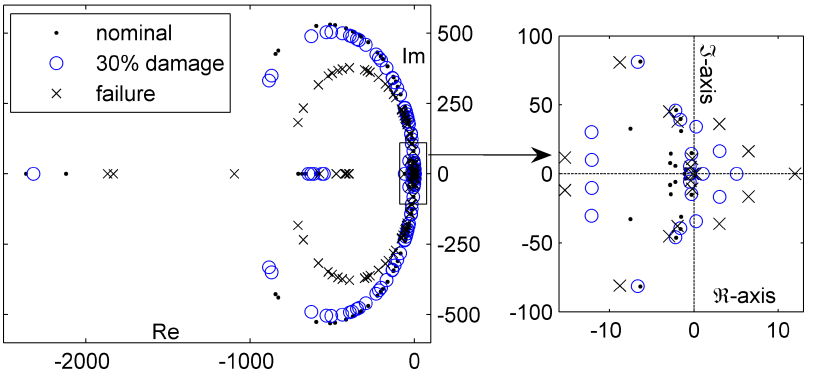

Fig. 12. Stability analysis of pole-placement scheme by closed-loop poles.

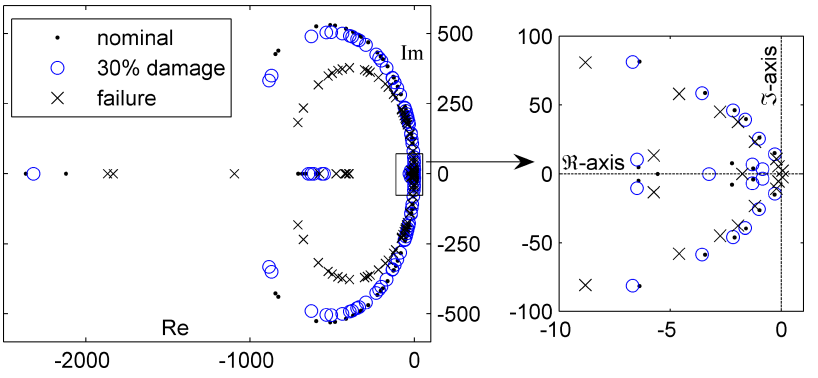

Fig. 13. Stability analysis of LQR scheme by closed-loop poles.

occur. To investigate the contribution of spill-over and uncertainty to the instability of the overall closed-loop system, let us analyze the closed-loop poles of the LQR system. As can be seen from Fig. 14 for the LQR system, neither the reduction spill-over, i.e. ROOB LQR (nominal), nor the damage uncertainty, i.e. full-state LQR (failure), can alone destabilize the system; but, when combined as shown in ROOB LQR (failure), they do.

Indeed, the LQR strategy using full-state feedback from the full-order model is highly robust to uncertainties (Ref. 33 demonstrates the significantly superior stability robustness of the full-state LQR compared with output feedback H_2, H_∞ and μ-synthesis controllers using a probabilistic approach). However, in practice, observation and reduction are inevitable and should be considered in control design. Reports on spill-over instability issues can be found in literature, e.g. see Ref. 34 as an early instance. Liu and Hou[35] proved that spill-over instability happens when both the control and observation spill-over terms are present. Therefore, spill-over instability can be avoided by eliminating either one, e.g. observation spill-over effect can be reduced utilizing low pass filters.[34] For attenuating the coupled effect of

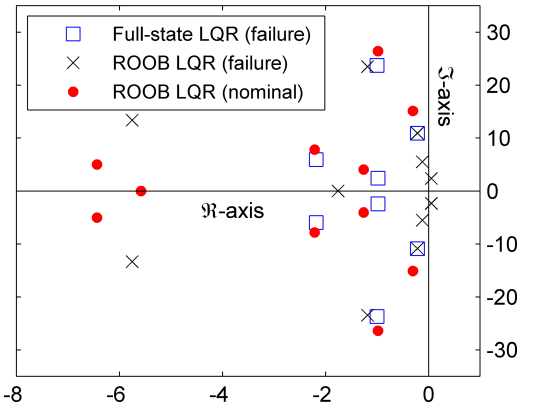

Fig. 14. Effect of spill-over and uncertainty on LQR stability.

spill-over and uncertainty (which is less emphasized in the literature), on the other hand, we could propose to treat the residual modes (eliminated in the reduction process) as norm-bounded uncertainties along with other present uncertainties within the framework of robust control. Of course, this approach would lead to new complexities and concerns such as high dimensionality of the controller (itself needing reduction) and degradation of nominal performance (too conservative design); furthermore, the stability robustness would be guaranteed only under the modeled uncertainty conditions. In the present investigation, these complexities are resolved exploiting the inherent robustness and simplicity of fuzzy control, and stability robustness is achieved as discussed in what follows.

The primary concern about the stability of the fuzzy controller system is because the FLC does not have a mathematical model to be used for stability analysis. Up to now although no general solution to this problem has been found, there is a number of stability analysis criteria proposed in the literature. One of these tests involves checking the ability of the controller to drive the system states to rest after the initial transient phase,[7] as shown in Fig. 15.

The stability test are performed considering the system with particular initial conditions on the state vector that seems to most severely excite the system and checking the ability of the FLC to reach equilibrium. Displacement and control force time histories, in Fig. 15, illustrate the ability of the GFLC to drive the system to rest from initial conditions in the nominal case and the two robustness tests.

6.2. *Performance robustness*

The term performance robustness implicitly implies the concept of stability robustness as a pre-requisite. Thus here only the LQR and GFLC performance robustness will be analyzed as the specific designed ROOB pole-placement looses stability in the tests.

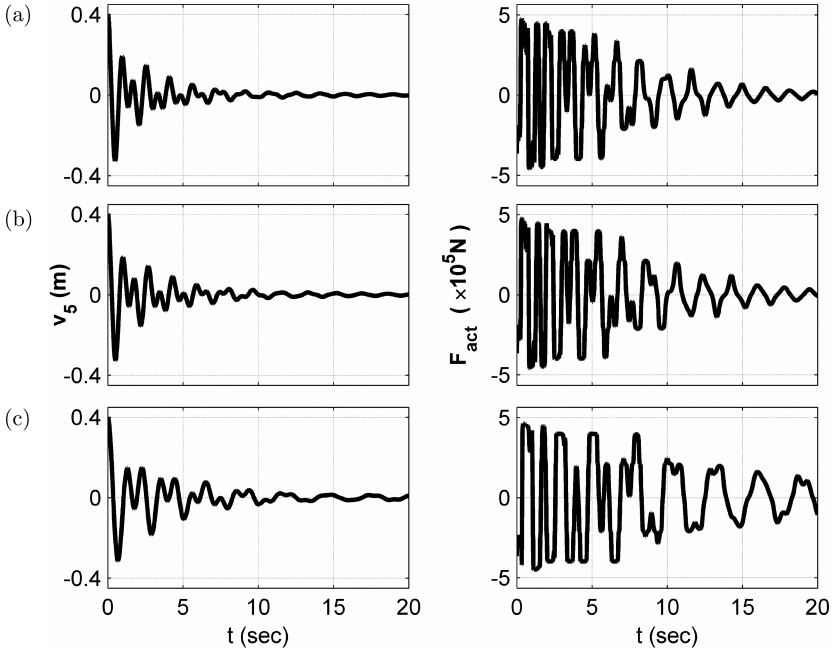

Fig. 15. Fuzzy stability tests in terms of displacement and control force(a) nominal, (b) 30% damage, (c) failure of the two members.

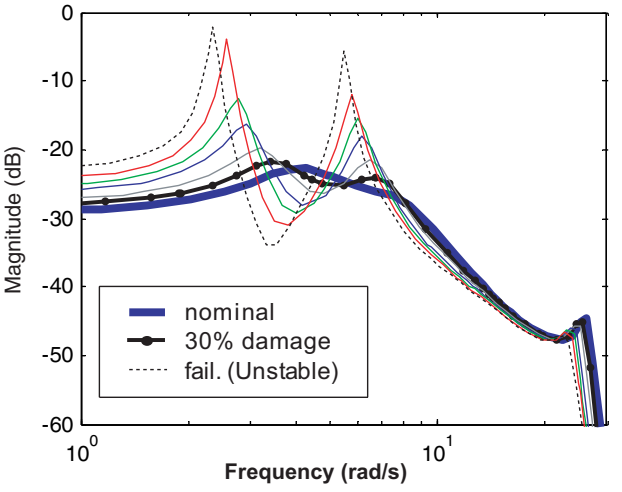

Fig. 16. Performance robustness analysis of LQR scheme by uncertain FRF.

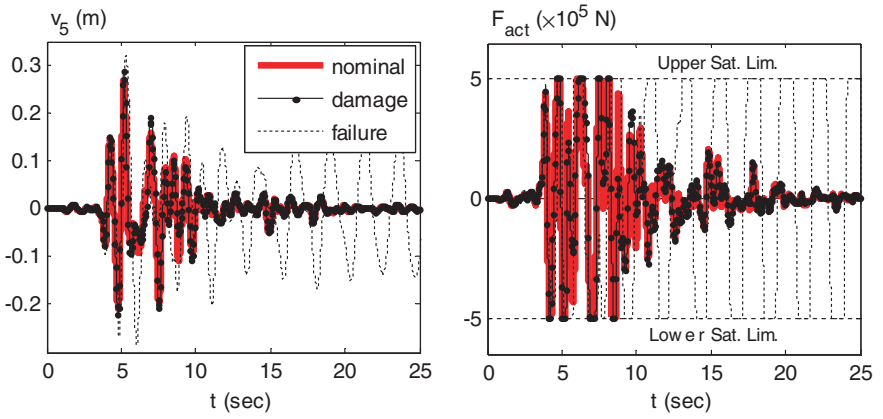

(a) (b)

Fig. 17. LQR scheme under robustness tests subjected to Kobe earthquake (a) displacement time-history, (b) control force time-history.

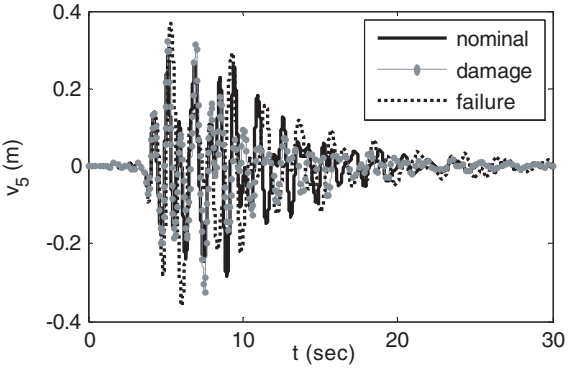

Fig. 18. GFLC under robustness tests subjected to Kobe earthquake.

Figure 16 shows the effect of $\{+0, -100\%\}$ uncertainty in the stiffness of the two members on the frequency response of the LQR control system. Figures 17 and 18 show the performance of LQR and GFLC control schemes subjected to robustness tests under the Kobe earthquake, while Table 6 presents complete numerical results of simulations associated with the proposed robustness tests. When comparing the performance data of a specific control in response to a specific loading for the three nominal/30% damage/failure cases, it should be noted that each is obtained through nondimensionalizing by its respective uncontrolled response. Hence, the last column of Table 6, as in case of Table 5, will prove to be useful for computing the peak and rms responses from the performance and rms ratios.

The pole-placement scheme in this investigation was merely a representative assignment of poles to show that a significant modification of closed-loop poles in the presence of uncertainties and spill-over effects may yield poor stability robustness

Table 6. Robustness tests results.

Test	Load	Performance[a][b]				Response[c][d]
		TMD	Pole Place.	LQR	GFLC	Unctrl
30% Damage of the two members	Elcentro	0.675[a]	Unstable	0.365	0.417	191
		0.498[b]		0.282	0.464	47.8
	Kobe	0.856		0.561	0.633	511
		0.761		0.424	0.795	90.5
	North Ridge	0.977		0.704	0.779	363
		0.525		0.465	0.687	109
	Weighted Ave.	0.875		0.587	0.656	
		0.618		0.417	0.693	
Failure of the two members	Elcentro	0.953	Unstable	Unstable	0.981	138
		0.812			0.639	46.3
	Kobe	0.680			0.535	684
		0.488			0.492	170
	North Ridge	0.723			0.500	767
		0.458			0.318	286
	Weighted Ave.	0.745			0.597	
		0.531			0.445	

Note: (a) Performance ratio Eq. (8-I), (b) rms ratio Eq. (8-II), (c) displacement peak (mm), (d) displacement rms (mm).

characteristics and lead to instability. The LQR scheme makes less modification to the closed loop poles and reaches approximately the same level of nominal performance while demonstrating much better robustness compared to the pole assignment example. This observation reveals that there are key points drastically influencing robustness that might remain neglected following a routine performance-based design.

The GFLC, on the other hand, although having slightly lower nominal performance, proves its unique robust stability and robust performance for the set of plants defined by the nominal structure under $\{+0, -100\%\}$ uncertainty in the stiffness of the two mostly stressed members.

Finally, it should be pointed out that by increasing the weighting R of the control effort in Eq. (10) a more robust LQR system would be obtained, e.g. using a value of 5e-14 instead of 1e-14 for R/Q in the present problem, the new LQR system would withstand the coupled instability effect of spill-over and uncertainty. However, the performance would be degraded (for the above example, the performance index (8-I) under nominal conditions would be reduced to 0.609 compared to the values of 0.532 and 0.551 for the original LQR and the GFLC, respectively) and there would be still no guarantee for stability of the closed-loop system under other uncertain conditions that are not checked. Accordingly, the GFLC remains the dominant design in terms of the compromise between performance and robustness.

7. Conclusions

In this paper, a GA-optimized fuzzy controller and output feedback reduced-order controllers based on pole-placement and LQR have been designed for vibration control of a seismically excited bridge structure, considering nominal performance and robustness. The stability and performance robustness of control schemes against model uncertainty due to damage is emphasized and simulation tests were conducted for numerical evaluation. It has been shown that there are certain advantages in employing intelligent controllers for structural control, including superior robustness and more convenience in handling design limitations and uncertainties. Results demonstrate that although an optimally designed conventional controller (utilizing accurate mathematical model of the linear system) can slightly surpass a fuzzy controller under ideal nominal conditions, it might demonstrate significant robustness disadvantages in practice. These robustness disadvantages, such as the instability issues due to the combined effect of spill-over and uncertainty, are only revealed if reduction and observation are taken into account in the design process to tackle inevitable practical limitations on available measurement and complexity of the models. On the other hand, these limitations are automatically resolved by fuzzy control.

It has been shown that fuzzy logic offers an inherent robust framework for structural control and can handle variations a standard controller might not withstand. Conventional controllers as those considered in this study, are intended to deliver optimal performance considering only nominal conditions. Even in conventional controllers designed based on the robust control theory which are explicitly intended to bear uncertainty, the practical usefulness is limited to the physical significance and relevance of the explicitly formulated uncertainty model and sources. Furthermore, robustness considerations in conventional controllers might result in conservative designs where nominal performance is sacrificed (the example provided in the last paragraph of Sec. 6.2 demonstrate that if the LQR controller is made to withstand the uncertainty as does the GFLC, its resulting nominal performance degradation would still keep it dominated by the GFLC). However, fuzzy controllers, exploiting mathematical model-free linguistic synthesis and nonlinearities, can be designed to deliver satisfactory nominal performance and superior robustness. The former property could be improved by GA optimization, as has been shown in this investigation, while the latter is achieved intrinsically without requiring the designer to get involved in complexities concerning explicit modeling of uncertainty.

References

1. K. Tanida, Progress in the application of active vibration control technologies to long-span bridges in Japan, *Prog. Struct. Engng Mater.* **4** (2002) 363–371.
2. S. V. Bakre and R. S. Jangid, Optimum multiple tuned mass dampers for base-excited damped main system, *Int. J. Struct. Stab. Dyn.* **4**(4) (2004) 527–542.
3. R. B. Carneiro, S. M. Avila and J. L. V. De Brito, Parametric study of multiple tuned mass dampers using interconnected masses, *Int. J. Struct. Stab. Dyn.* **8**(1) (2008) 187–202.

4. C. Li, B. Han, J. Zhang, Y. Qu and J. Li, Active multiple tuned mass dampers for reduction of undesirable oscillations of structures under wind loads, *Int. J. Struct. Stab. Dyn.* **9**(1) (2009) 127−149.
5. K. B. Lim, Robust control of vibrating structures, in *Responsive Systems for Active Vibration Control*, ed. A. Preumont (Kluwer Academic Publishers, Netherlands, 2002), pp. 133−179.
6. L. A. Zadeh, Fuzzy sets, *Information and Control.* **8** (1965) 338−353.
7. M. Al-Dawod, B. Samali, F. Naghdy and K. C. S. Kwok, Active control of along wind response of tall building using a fuzzy controller, *Engng. Struct.* **23** (2001) 1512−1522.
8. A. S. Ahlawat and A. Ramaswamy, Multi-objective optimal design of FLC driven hybrid mass damper for seismically excited structures. *Earthquake Engng Struct. Dyn.* **31** (2002) 1459−1479.
9. Q. Lu, P. Zhike, F. Chu and J. Huang, Design of fuzzy controller for smart structures using genetic algorithms, *Smart Mater. Struct.* **12**(6) (2003) 979−986.
10. H. S. Kim and P. N. Roschke, Design of fuzzy logic controller for smart base isolation system using genetic algorithms, *Engng. Struct.* **28**(1) (2006) 84−96.
11. S. Pourzeynali, H. H. Lavasani and A. H. Modarayi, Active control of high rise building structures using fuzzy logic and genetic algorithms, *Engng. Struct.* **29** (2007) 346−357.
12. A. I. Dounis, P. Tiropanis, G. P. Syrcos and D. Tseles, Evolutionary fuzzy logic control of base-isolated structures in response to earthquake activity, *Struct. Control Health Monit.* **14** (2007) 62−82.
13. D. A. Shook, P. N. Roschke, P. Y. Lin and C. H. Loh, GA-optimized fuzzy logic control of a large-scale building for seismic loads, *Engng. Struct.* **30** (2008) 436−449.
14. H. N. Li and D. H. Zhao, Control of structures with semi-active friction damper by intelligent algorithm, in *2006 IEEE International Conference on Fuzzy Systems*, Vancouver, BC, Canada (July 16−21, 2006).
15. R. Guclu and H. Yazici, Vibration control of a structure with ATMD against earthquake using fuzzy logic controllers. *J. Sound Vib.* (2008).
16. D. A. Linkens and H. O. Nyonggesa, Genetic algorithm for fuzzy control-part 1: Offline system development and application, in *IEE Proc. on Control Theory Application.* **142** (1995) 161−176.
17. D. A. Linkens and H. O. Nyonggesa, Genetic algorithm for fuzzy control-part 2: Online system development and application. *IEE Proc. on Control Theory Application.* **142** (1995) 177−185.
18. J. D. Yau and Y. B. Yang, A wideband MTMD system for reducing the dynamic response of continuous truss bridges to moving train loads, *Engng. Struct.* **26** (2004) 1795−1807.
19. H. N. Li, S. Y. Dong and Y. U. Li, Optimum spatial placement of dampers in vibration controlled structures based on genetic algorithms, *J. Vib. Shock.* **25**(2) (2006) 1−4.
20. Y. Fujino and M. Abe, Design formulas for tuned mass dampers based on a perturbation technique, *Earthquake Engng. Struct. Dyn.* **22** (1993) 833−854.
21. K. Glover, All optimal Hankel norm approximation of linear multivariable systems, and their $L\infty$- error bounds, *Int. J. Control.* **39**(6) (1984) 1145−1193.
22. J. C. Wu, J. N. Yang and W. E. Schmitendorf, Reduced-order H∞ and LQR control for wind-excited tall buildings, *Engng. Struct.* **20**(3) (1997) 222−236.
23. G. Obinata and B. D. O. Anderson, *Model Reduction for Control System Design.* (Springer-Verlag, London, 2001).
24. S. Pourzeynali and T. K. Datta, Control of suspension bridge flutter instability using pole-placement technique, *J. Sound Vib.* **282** (2005) 89−109.
25. P. C. Wang, F. Kozin and F. Amini, Vibration control of tall buildings, *Engng. Struct.* **5** (1983) 282−289.

26. K. Ogata, *Modern Control Engineering*, 4th edn. (Prentice Hall, New Jersey, 2002).
27. H. T. Nguyen, Neural networks and fuzzy logic, Technical Notes, University of Technology, Sydney (1998).
28. L. Wang and J. Mendel, Generating fuzzy rules by learning from examples, *IEEE Trans on System, Man, and Cybernetics.* **22**(6) (1992) 1414−1427.
29. E. Dehghan-Niri, S. M. Zahrai and A. Mohtat, Effectiveness-robustness objectives in MTMD system design: An evolutionary optimal design methodology, *Struct. Control Health Monit.* (2008).
30. E. H. Mamdani and S. Assilian, An experiment in linguistic synthesis with a fuzzy logic controller, *Int. J. of Man-Machine Studies.* **7**(1) (1975) 1−13.
31. D. E. Goldberg, *Genetic Algorithms in Search, Optimization and Machine Learning.* (Addison-Wesley, MA, 1989).
32. J. Yan, M. Ryan and J. Power, *Using Fuzzy Logic* (Prentice Hall Inc, 1994).
33. Jr. R. V. Field, P. G. Voulgaris and L. A. Bergman, Probabilistic stability robustness of structural systems, *Journal of Engng. Mech.* **122**(10) (1996) 1012−1021.
34. M. J. Balas. Feedback control of flexible systems, *IEEE Transactions on AC.* AC-**23**(4) (1978) 673−679.
35. W. Liu and Z. Hou, A new approach to suppress spillover instability in structural vibration control, *Struct. Control Health Monit.* **11** (2004) 37−53.